

S. MRÓZ^{##}, A. STEFANIK^{*}, P. SZOTA^{*}, M. KWAPISZ^{*}, M. WACHOWSKI^{**},
L. ŚNIEŻEK^{**}, A. GAŁKA^{***}, Z. SZULC^{***}

NUMERICAL AND EXPERIMENTAL MODELING OF PLASTIC DEFORMATION THE MULTI-LAYER Ti/Al/Mg MATERIALS

The paper has presented the results of theoretical studies and experimental tests of the plastic deformation of multi-layered Ti/Al/Mg specimens. Theoretical studies were carried out using the Forge2011[®] computer program. Physical modeling, on the other hand, was performed using the Gleeble3800 simulator. Cuboidal specimens were cut off from the plates obtained in the explosive welding method. Based on the obtained investigation results it has been found non uniform deformation of the particular layer as a result their different value of flow stress.

Keywords: multi-layered Ti/Al/Mg material, plastic deformation, physical modelling, numerical modelling

1. Introduction

Traditional combat vehicle armours are usually manufactured as either monolithic or multilayered from high-strength steel plates [1-3]. Armours of this type are characterized by high specific weight and cannot be used in aircraft or helicopters. Therefore, new solutions are being sought for, which will be based on materials providing high ballistic protection, while having the lowest possible specific weight. Such solutions may include multilayered armours made of low-density materials [4-6]. Armours of this type are composed of several layers of different metals of materials that perform a specific role in destroying a missile and absorbing the impact energy. To achieve a low armour mass, ceramic materials, plastics or fibre-reinforced epoxy resins are used [7-9]. Whereas, of metallic materials other than steel, high-strength aluminium and titanium alloys are being increasingly often used for the construction of such armours [10-12].

Combat aircraft is equipped with a number of electronic devices. Each electronic device is a source of electromagnetic radiation which, according to needs, can be regarded as either a desirable phenomenon or a side effect of the device's operation [13]. In the case of military technology, electromagnetic radiation is an undesirable phenomenon as it increases the probability of a vehicle or aircraft being detected on a potential battlefield. To reduce such a risk, screens are used to shield the electromagnetic field interaction. Materials used for such screens include mainly heavy metals (steel, copper and nickel) or various types of polymer composites [16]. Due to the large specific weight of the above-mentioned metals, their use in combat aircraft is

impractical or, in some cases, impossible. Studies [17-19] have shown that materials that have also high electromagnetic field shielding ability are magnesium alloys. However, a prerequisite in this case is to achieve the appropriate properties of the structure which can be obtained as a result of plastic deformation or ageing. Study [19] has shown that the 60% deformation of AZ31 alloy plate, achieved in a rolling process, guarantees an increase in resistance to electromagnetic field radiation at a level that is required in the armaments industry.

Available technical literature lacks information concerning lightweight metallic multilayered armours that provide high ballistic protection and electromagnetic field shielding ability at the same time. A response to the aforementioned challenges is the development of a new multilayered Ti/Al/Mg material, in which the Ti/Al layers offer an increased ballistic resistance and will constitute a constructional material, while the layer made of the magnesium alloy will be responsible for electromagnetic field shielding. However, producing this material involves the solution of a number of technological and constructional problems, from the selection of materials that meet specific design criteria through to the choice of the technology of joining so different metals into a multilayered material. One of the few methods which enable bonding of metallic materials differing in mechanical properties or density is explosive welding [20-22]. This method enables the production of multilayered materials that are characterized by high bond strength, which is indispensable in the case of ballistic shields. The selection of materials in terms of strength and ballistic resistance, which will perform the constructional function in multilayered laminate, i.e. the aluminium

* CZESTOCHOWA UNIVERSITY OF TECHNOLOGY, FACULTY OF PRODUCTION ENGINEERING AND MATERIALS TECHNOLOGY, 19 ARMII KRAJOWEJ AV., 42-201 CZESTOCHOWA, POLAND

** MILITARY UNIVERSITY OF TECHNOLOGY, FACULTY OF MECHANICAL, 2 GEN. SYLWESTRA KALISKIEGO STR., 00-908 WARSZAWA 46, POLAND

*** ZTW EXPLOMET SP.J. 100 OŚWIECIMSKA STR., 46-020 OPOLE, POLAND

Corresponding author: mroz@wip.pcz.pl

and titanium alloys, is defined in the authors' earlier publications [23,24]. While magnesium alloy AZ31, as a material providing protection against electromagnetic radiation, was selected based on study [19]. As has been mentioned above, obtaining the appropriate electromagnetic field shielding ability by alloy AZ31 requires its deformation. The deformation of the Mg layer may not take place before explosive welding, because due to its poor plasticity, this layer would be destroyed during the course of explosive welding. For explosive welding, the magnesium alloy should be annealed to a softened condition. For this reason it is necessary to determine the plastic working parameters for the obtained Ti/Al/Mg multilayered material from a multi-stage investigation process that will include the determination of the temperature, speed or the preset deformation [25,26].

The aim of the study was to determine the effect of process parameters (mainly temperature) on the deformability of the Ti/Al/Mg material. The paper reports the results of theoretical studies and experimental testing of the plastic deformation and flow of the new Ti/Al/Mg multilayered material. Physical modeling was performed using the Gleeble3800 simulator. While the theoretical studies were carried out using the Forge® computer program.

2. Materials and testing methodology

The Ti/Al/Mg multilayered materials was obtained by the explosive welding method. For explosive welding, 3 sets of specimens were prepared, each composed of plates made of magnesium

alloy AZ31 (the base layer), plates of an aluminium alloy in grade AA2519 (cladding layer A) and plates of a titanium alloy in grade Ti6Al4V (cladding layer B). The thickness of individual plates was approx. 5 mm. Since the aluminium and titanium alloy plates used are characterized by high hardness, while the magnesium alloy plate is hard deformable at ambient temperature, which could give rise to cracks forming at the joint boundary during explosive welding, additional "technological separators" made of AA1050 grade aluminium were employed in the explosive welding process (in one step). The thickness of these separators was 0.5 mm. The explosive-welding process was performed in the EXPLOMET High-Energy Techniques Works, a Polish company concerned with explosive metalworks. As an explosive material, a mixture of ammonium nitrate fuel oil (ANFO) was used. A parallel configuration of the welding system was used to achieve a bond. The scheme of the explosive-welding system is presented in Fig. 1. The detonation speed was equal to 2200 m/s.

Multilayered plates of dimensions of $250 \times 100 \times 15.3$ mm were obtained from explosive welding. The obtained plates exhibited a slight bend towards the titanium layer. No delaminations nor discontinuities were observed at the joint boundary between individual components. The deformability of the material used was examined in compression tests on $10 \times 15 \times 20$ mm cuboid specimens which had been cut out along the single-layer plate (the area marked in red in Fig. 2).

The shape of an example specimen used in physical modeling is shown in Fig. 3. For theoretical studies using a FEM-based software program, appropriate geometrical models were made (Fig. 4a).

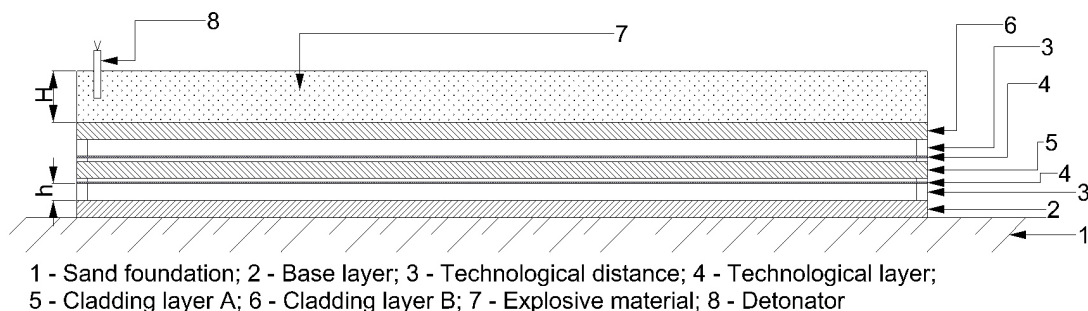


Fig. 1. Scheme of the explosive welding system

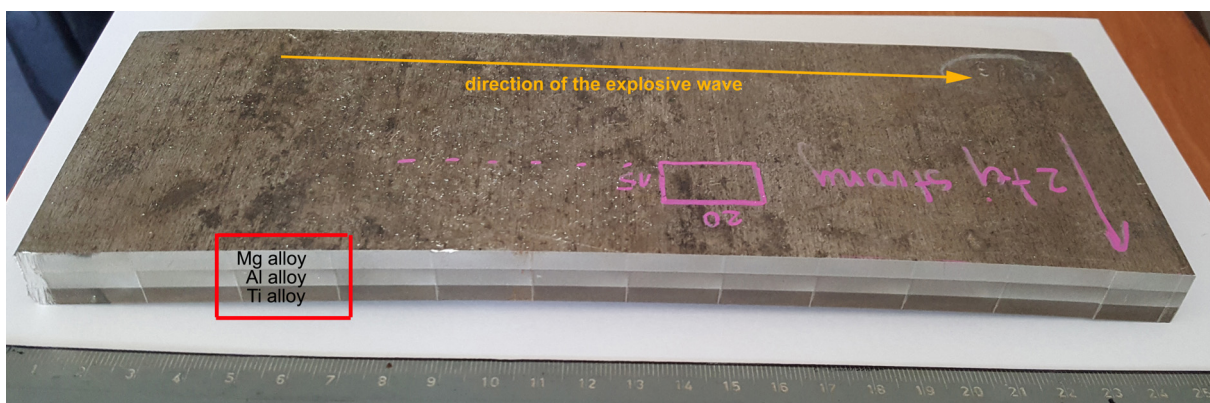


Fig. 2. A view of the multi-layer plate after the explosive welding

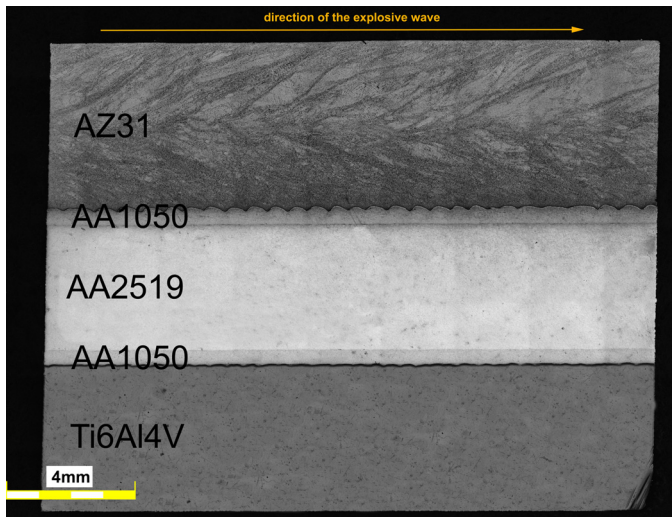


Fig. 3. A view of the Ti/Al/Mg specimen used for the physical modeling

The forming behavior of the particular layer in the Ti/Al/Mg material was studied using compression tests performed with a Gleeble3800 system. The schedule of the compression test is shown in Fig. 4.

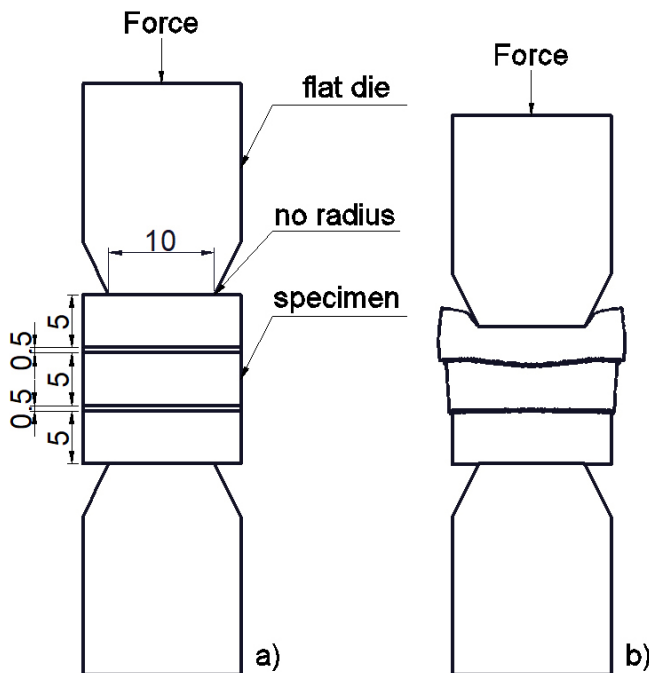


Fig. 4. The schedule of compression test using the Gleeble3800 simulator – a) and the view of the specimen after deformation – b)

The following parameters were adopted for the numerical and physical modeling: true strain, 0.17; tool velocity, 1 mm/s, and temperature, 300°C, 350°C and 400°C. The temperature range was chosen based on the authors' earlier studies [26] concerning the process of Mg/Al bimetal metal forming. The physical modeling of the cuboidal Ti/Al/Mg specimen compression test were made for the verify results of the numerical modeling.

The thermo-mechanical simulation of the compression tests was carried out with the use of a visco-plastic model in

the triaxial state of strain by using the Forge2011[®] program, whereas the properties of the deformed material were described according to the Norton-Hoff [27,28] conservation law. The application of the computer program Forge2011[®] using the thermo-mechanical models that it contains requires the definition of boundary conditions which are decisive to the correctness of numerical computation. The properties of individual bimetallic components have been determined in the authors' previous studies [29] (for AZ31 alloy and aluminium AA1050). The properties of the aluminium alloy grade AA2519 and titanium alloy grade Ti6Al4V have been taken from the material data base of computer program Forge2011.

For numerical computations, the Coulomb and the Tresca mixed friction model was adopted; the value of the friction coefficient was assumed to be 0.08, while that of the friction factor, 0.15 [30]. The use of the explosive welding method for making bimetallic stocks ensures a firm bond of the components to be achieved. Thus, in numerical simulations, the bond between the particular cladding layers was defined as firmly adhering. The nodes of both meshes were not connected. In order to increase the speed and accuracy of computations, $\frac{1}{4}$ of the bimetallic specimen cross-section were used in the simulations.

3. Results and discussion

At the first investigation stage, the correctness of the initial and boundary parameters adopted for numerical simulations were verified by comparing the variation of forces necessary for the deformation of multilayered Ti/Al/Mg specimens as a function of displacement. The results obtained from numerical computations and recorded during physical modeling are shown in Fig. 5.

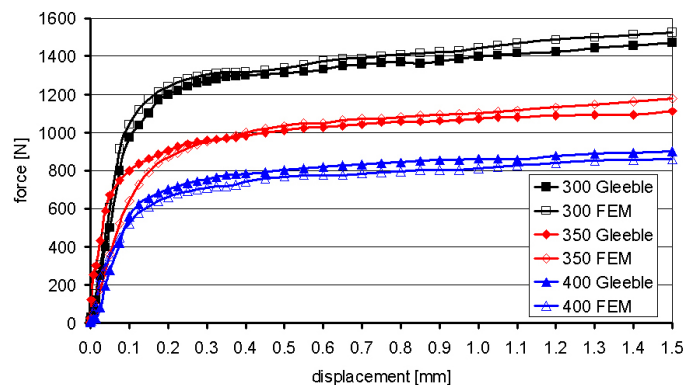


Fig. 5. Force vs. displacement curves obtained from compression tests of Ti/Al/Mg specimens

The data represented in Fig. 5 shows that, regardless of the temperature at which Ti/Al/Mg specimen testing was conducted, high consistence, both qualitative and quantitative, was obtained within the entire deformation range. This bears evidence of the correct definition of the numerical simulation parameters. Moreover, as expected, the increase in temperature resulted in a decrease in force necessary for deformation, which is due to

a reduction in the value of plastic flow stress in individual layers of the multilayered material. The largest differences in forces were noted when increasing the temperature from 300 to 350°C, with a force drop at the maximum displacement by as much as 25%. While increasing the temperature from 350 to 400°C resulted in a force drop by approx. 20%. The difference in force for the extreme temperature values amounted to approx. 40%. Analysis of the obtained maximum force values shows a significant effect of the temperature, at which specimen compression was conducted. The obtained data will be helpful in the design of rolling technology (selection of the process temperature) for the Ti/Al/Mg material under examination.

At the next stage of the study, analysis of the distributions of strain, stress and plastic flow in individual layers was made using the computer simulation results. Whereas, the effect of the technological layer on the obtained distribution of the parameters under examination was not analyzed in the study. In view of the fact that the variations in force as a function of displacement, represented in Fig. 5, enable the evaluation of the effect of temperature on the plastic flow stress of the material under investigation only in a rough (indirect) manner, the distribution of stress intensity on the cross-section was compared for individual layers of the investigated Ti/Al/Mg material (Fig. 6).

Figure 6 shows that the obtained stress intensity distributions in individual layers are non-uniform and differ in obtained stress values. Whereas, the greatest flow stress values were obtained for the lowest temperature, while the smallest, for the highest temperature, which results directly from the behaviour of the plastic flow curves for respective components of the material under analysis [26,29].

One of the objectives set in the study was to select the temperature parameters that would provide the most uniform possible deformation of individual layers. For individual components of the examined material, due to substantial differences in mechanical properties, this is practically impossible. Therefore, attention should be focused on the selection of temperature parameters such that the obtained plastic flow stress values for individual components are the closest possible to one another,

which will contribute to increasing the uniformity of deformation of the layers. When analyzing the data in Fig. 6a it can be noticed that the smallest differences in average stress intensity values were obtained at the temperature 300°C (the Ti layer – approx. 180 MPa, the Al layer – approx. 150 MPa, and the Mg layer – approx. 100 MPa, with the difference in average values being 80 MPa). While the largest differences were noted at the highest temperature, i.e. 400°C (the Ti layer – approx. 150 MPa, the Al layer – approx. 70 MPa, and the Mg layer – approx. 40 MPa, with the difference in average values being greater than 100 MPa), Fig. 6c. Thus, it can be inferred that using the temperature 300°C should provide a more uniform deformation of individual layers of the investigated material. Figure 6 implies also, regardless of preset temperature, a local increase in stress intensity for outer layers, which is especially well visible for the Ti alloy at the location of contact between the anvil and the layer. This is associated with the prevailing conditions of friction on the surface of the deformed materials and with the loading pattern. The assumed deformation temperatures, while for the Mg and Al layers falling within the range of hot plastic working for these alloys, for the Ti layer fall within the “warm” plastic working range, which causes the generation of larger stress values. In this case, the anvil edges cause a “notch phenomenon” to occur in the material, thus giving rise to stress concentration.

The obtained stress intensity values affect the deformability of individual layers. Figure 7 shows the strain intensity distribution for the assumed temperature parameters.

It can be seen from Fig. 7 that the variation in temperature significantly influences the obtained strain intensity distributions and contributes to a reduction of deformation non-uniformity for individual layers. With the increase in temperature, the deformation of the middle AA2519 alloy layer decreases at the expense of an increase in the deformation of the Mg alloy layer. Moreover, for the lowest temperature, a slight deformation of the Ti layer (a bend of the free specimen part not contacting with the anvil) was observed. Also the deformation of the technological separator is the greatest for this temperature, which suggests

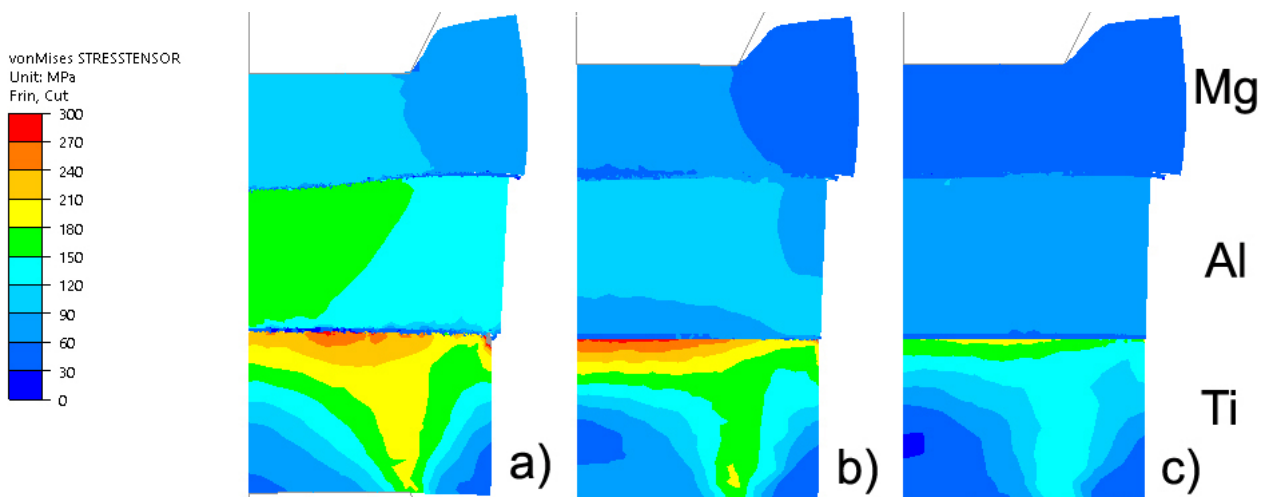


Fig. 6. Distribution of effective stress in the Ti/Al/Mg specimens after compression tests: a) 300°C, b) 350°C, c) 400°C, (1/2 of the specimen)

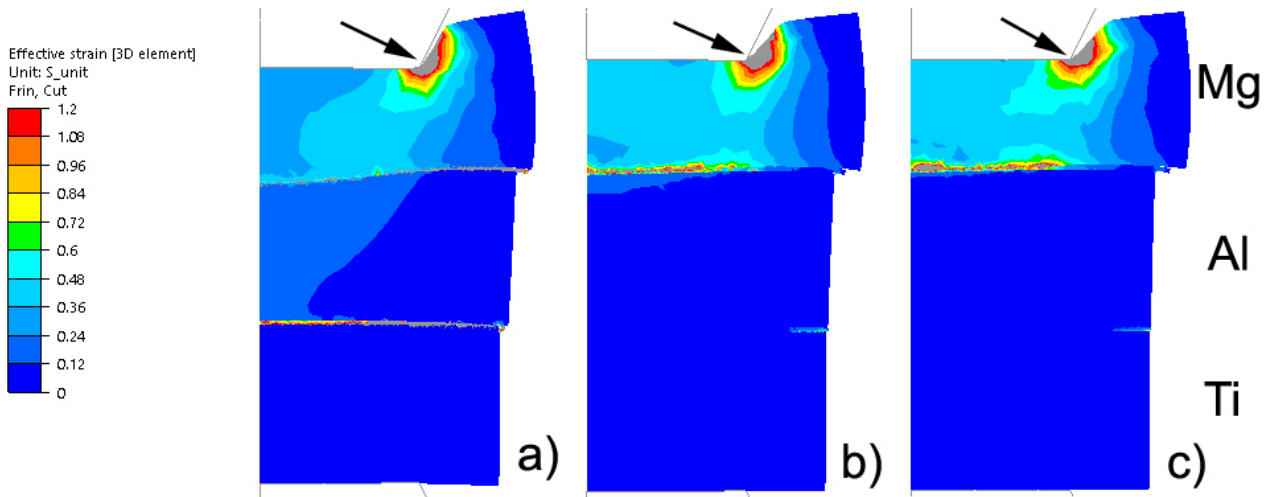


Fig. 7. Distribution of effective strain in the Ti/Al/Mg specimens after compression tests: a) 300°C, b) 350°C, c) 400°C, (1/2 of the specimen)

the penetration of the deformation into the Ti layer. As has been mentioned above, with increasing temperature the middle Al layer and the outer Ti layer practically do not deform and start acting on the AZ31 alloy layer as rigid tools, causing an increase in deformation non-uniformity. In the figure under examination, an Mg alloy layer region is also marked, which is subject to action of the sharp anvil portion that causes a rapid increase in strain values (going beyond the range of the scale). According to the results of study [26], the distribution of strains with significant values, being characteristic of that region, gives rise to the occurrence of additional shear bands, which will contribute to structure refinement. A detailed structural analysis for those regions will be the subject of further investigation.

The non-uniform distribution of strain and flow stress at the height of deformed specimens influences the plastic flow of individual layers. Figure 8 shows the distribution of the vertical component, v_y , in respective layers as a function of preset deformation temperature.

The obtained numerical computation results have definitely confirmed the effect of temperature on the flow of individual components. The horizontal lines marked in Fig. 8 are super-

imposed in the plane, in which the metal does not move in the vertical direction (the neutral line – zero flow velocity in the direction under analysis). For the conditions, for which individual layers flow uniformly in the vertical direction, these lines should be positioned in the horizontal axis of symmetry of the specimen. In the case under analysis, the position of these lines is shifted towards a more deformed layer, in this case the AZ31 alloy. Whereas, the position of a neutral line being the closest to the horizontal axis of symmetry was noted for the lowest temperature (Fig. 8a). As the temperature increases, the neutral line moves towards the upper anvil, which is indicative of a larger deformation of the outer Mg layer, as compared to the other two layers. A further increase in temperature to 400°C does not significantly changes the neutral line position, compared to the temperature 350°C.

Considering the fact that in the compression test a decisive role is played by compressive stresses in the direction of reduction, an additional analysis of variations in the stress component σ_y in the analyzed direction was made in the study. Figure 9 shows the distribution of σ_y stress as dependent on the temperature, at which the experiment was run.

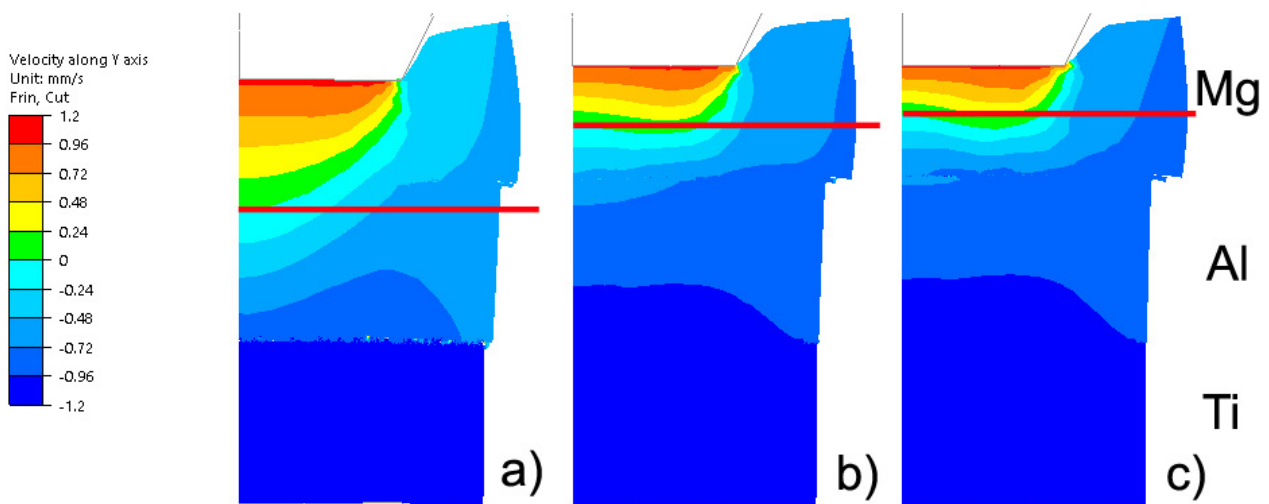


Fig. 8. Distribution of the vertical velocity v_y in the Ti/Al/Mg specimens after compression tests: a) 300°C, b) 350°C, c) 400°C, (1/2 of the specimen)

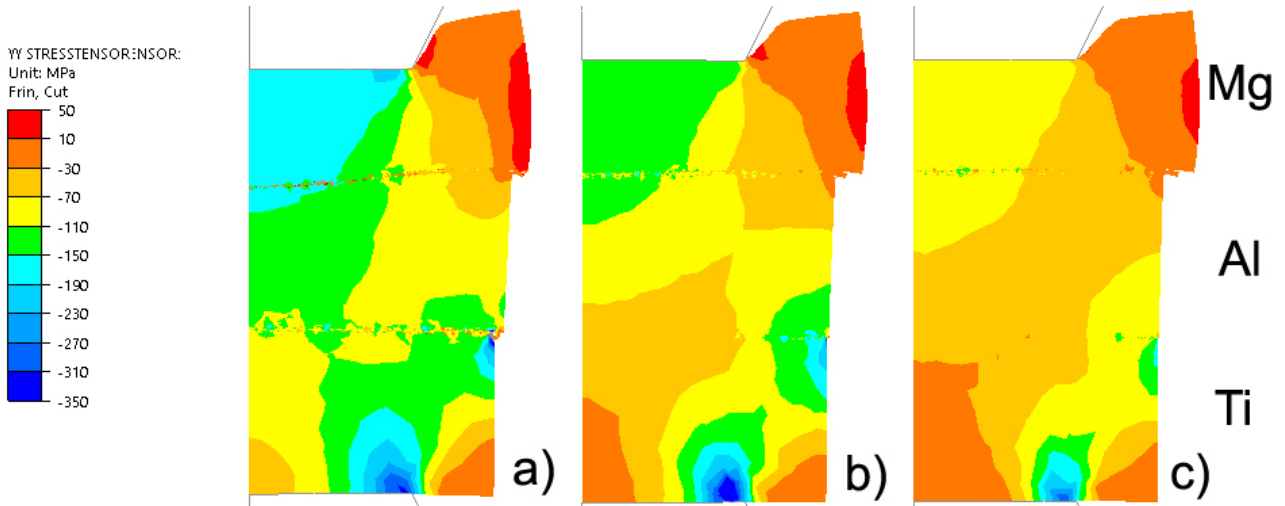


Fig. 9. Distribution of the vertical stress σ_y component in the Ti/Al/Mg specimens after compression tests: a) 300°C, b) 350°C, c) 400°C, (1/2 of the specimen)

The data in Fig. 9 suggests that, regardless of the preset temperature value, compressive stresses predominate in the specimen regions undergoing the action of the flat anvil parts. Whereas, as the temperature increases, their value in the AZ31 layer decreases, while in the middle Al layer and the Ti layer it starts approaching zero. This confirms the fact of the reduction in the deformation of these layers with the increase in temperature. For the Ti layer, a considerable concentration (increase) of compressive stress values was observed in the sharp anvil end region, regardless of the preset temperature value. The obtained distribution is consistent with the data shown in Fig. 6. In the case of free parts situated beyond the direct action of the flat anvil portion, a change in stress distribution character from compressive stress to tensile stress occurred for the Mg alloy. This is especially visible for the lowest temperature (Fig. 9a). It is a very unfavourable phenomenon, because a considerable stress gradient arises within a small region, which, in extreme cases, may result in a loss of metal integrity. In the case at hand, it results from the transverse displacement of the Mg layer beyond the middle Al layer. In this case, the Al layer acts as an undeformable tool.

To verify the obtained numerical computation results, an analysis of variations in the shape of individual layers deformed

at different temperatures was made. Figures 10 and 11 illustrate the analysis of dimensional variations for individual Ti/Al/Mg layers of the material.

The data represented in Figs. 10 and 11 shows that the increase in temperature is followed by an increase in deformation of the AZ31 alloy layer (the greatest reduction in its height) at the free surface of the remaining layers. In addition, the most intensive displacement of the Mg layer in the transverse direction can be observed at the lowest temperature (Fig. 10a), compared to the conditions where higher temperatures were applied (Figs. 10b & 10c). A detailed analysis of the data in Fig. 11 confirmed the obtained strain intensity distributions shown in Fig. 7. No deformation of the Ti layer at the temperatures 350 and 400°C and a slight deformation for 300°C. As a result of physical modeling, the middle layer deformed to a similar extent. On the other hand, according to the numerical computation results, the greatest differences in thickness were noted for the layer made of the Mg alloy.

The data in Fig. 10a shows also that the unfavourable distribution of tensile stresses for the free portion of the magnesium alloy layer (Fig. 9a) caused a loss in the integrity of this layer at the location where a tensile stress gradient occurred. The trans-

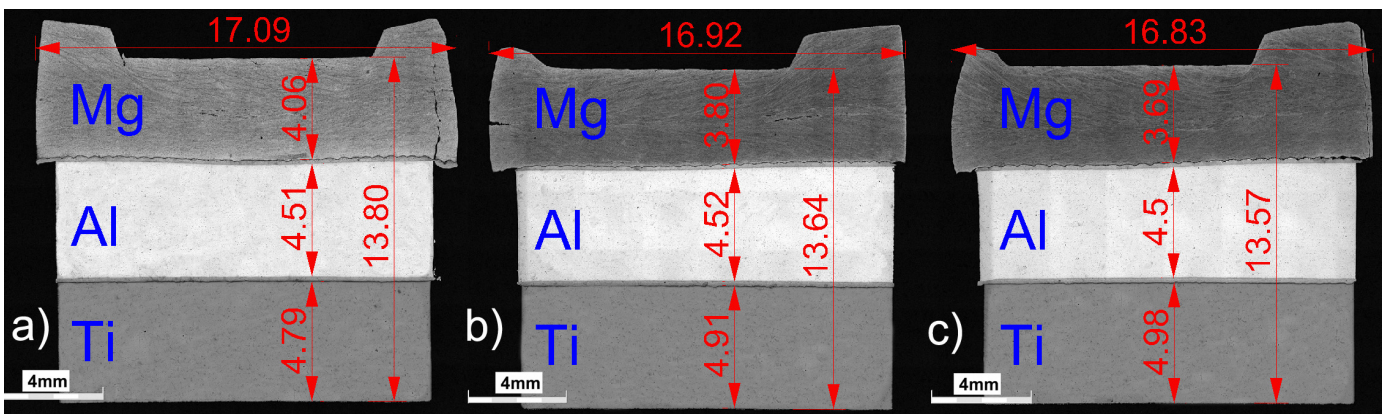


Fig. 10. A view of the specimens cross-section after compression tests: a) 300°C, b) 350°C, c) 400°C

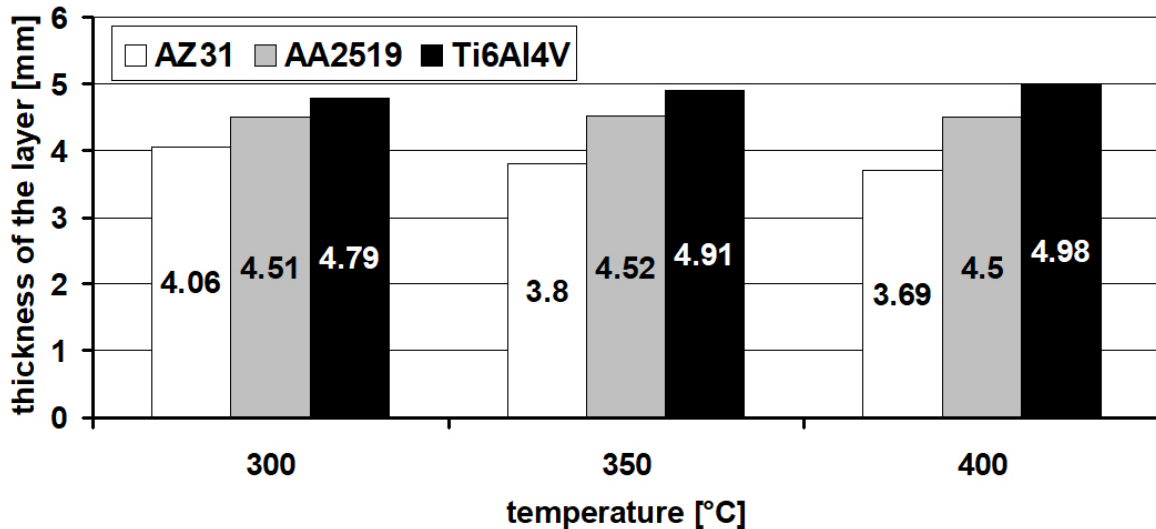


Fig. 11. Comparison of variations in the thickness of individual layers in the examined Ti/Al/Mg material

verse flow of individual layers takes place through the employed technological separators of soft aluminium, which in this case act as a lubricant. Increasing the temperature to 400°C resulted also a delamination at the boundary of the joint between the outer Mg layer and the middle layer. One of the physical causes might be the formation of intermetallic phases between these layers, which are hard and brittle, thus causing a weakening of the joint, as has been shown in the authors' earlier study [31]. Detailed structural examinations will be part of further investigations by the authors.

4. Summary

The investigation has demonstrated that the uniform flow of the multilayered Ti/Al/Mg material is hampered or even impossible due to considerable differences in the values of plastic flow stress of individual material components. This makes the final height of individual layers vary. To obtain a Ti/Al/Mg material that will exhibit an identical final height of individual layers, the starting material should be made with a varying height of individual layers. The selection of the deformation temperature for these types of multilayered materials may, to a small extent, reduce the non-uniformity of deformation of individual layers.

Acknowledgements

The part of research was funded by Polish Ministry of National Defence, grant number: BG/13-998.

REFERENCES

- [1] A. Wiśniewski, *Pancerze – budowa, projektowanie i badanie*, WNT, Warszawa (2001).
- [2] W. Gooch, M. Burkins, R. Squillaciotti, R. Stockmannkoch, H. Oscarsson, C. Nash, *Ballistic Testing of Swedish Steel ARMOX Plate for U.S. Armor Applications*, 21st International Ballistic Symposium, Adelaide Australia, 19-23 April 2004.
- [3] T. Børvik, S. Dey, A.H. Clausen, *Perforation resistance of five different high-strength steel plates subjected to small-arms projectiles*, *Int. J. Impact Eng.* **36**, 948-964 (2009).
- [4] J. Godzimirski, J. Janiszewski, M. Rośkiewicz, Z. Surma, *Ballistic resistance tests of multi-layer protective panels*, *Maint. and Reliab.* **17** (3), 416-421 (2015).
- [5] A. Tasdemirci, I.W. Hall, *Development of novel multilayer materials for impact applications: A combined numerical and experimental approach*, *Mater. Des.* **30**, 1533-1541 (2009).
- [6] B. Płonka, K. Remsak, M. Rajda, *Badania balistyczne demonstratorów opancerzenia dodatkowego*, *Szybk. Poj. Gąsien.* **47** (1), 1-10 (2018).
- [7] Z. Odanović, B. Bobić, *Ballistic protection efficiency of composite ceramics/metal armours*, *Scient.-Techn. Rev.* **3**, 30-38 (2003).
- [8] S. Atiq, A.R. Boccaccini, D.N. Boccaccini, I. Dlouhy, C. Kaya, *Fracture behaviour of mullitefibre reinforced-mullitematrix composites under quasi-static and ballistic impact loading*, *Comp. Sc. and Techn.* **65**, 325-333 (2005).
- [9] T.A. Bogetti, B.A. Cheeseman, *Ballistic impact into fabric and compliant composite laminates*, *Comp. Struct.* **61**, 161-173 (2003).
- [10] K.O. Pedersen, T. Børvik, O.S. Hopperstad, *Fracture mechanisms of aluminium alloy AA7075-T651 under various loading conditions*, *Mater. Des.* **32**, 97-107 (2011).
- [11] T. Børvik, O.S. Hopperstad, K.O. Pedersen, *Quasi-brittle fracture during structural impact of AA7075-T651 aluminium plates*, *Int. J. Impact Eng.* **37**, 537-551 (2010).
- [12] D. Boroński, M. Kotyk, P. Maćkowiak, L. Śnieżek, *Mechanical properties of explosively welded AA2519-AA1050-Ti6Al4V layered material at ambient and cryogenic conditions*, *Mater. Des.* **133**, 390-403 (2017).
- [13] L. Szugajew, J. Jarzowski, *Niektóre aspekty konstrukcji powłok ekranujących i absorpcyjnych – część II*, *Probl. Techn. Uzbr.* **36** (104), 121-127 (2007).

- [14] D.R.J. White, *Electromagnetic Shielding Materials and Performance*, Don White Consultants Inc., USA, 1980.
- [15] T. Chen-Ching, Ch. Chien-Chih, *Experimental Data for Study on the Shielding Effect of Electromagnetic Wave*, *Eng.* **3**, 771-777 (2011).
- [16] L.N. Kong, Z.W. Li, L. Liu, R. Huang, M. Abshinova, Z.H. Yang, Recent progress in some composite materials and structures for specific electromagnetic applications, *Int. Mater. Rev.* **58**, 203-59 (2013).
- [17] X. Chen, J. Liu, Z. Zhang, F. Pan, Effect of heat treatment on electromagnetic shielding effectiveness of ZK60 magnesium alloy, *Mater. Des.* **42**, 327-333 (2012).
- [18] X. Chen, J. Liu, F. Pan, Enhanced electromagnetic interference shielding in ZK60 magnesium alloy by aging precipitation, *J. of Phys. and Chem. of Sol.* **74**, 872-878 (2013).
- [19] K. Song., F.S. Pan, X.H. Chen, Z.H. Zhang, A.T. Tang, J. She, Z.W. Yu, H.C. Pan, X.Y. Xu, Effect of texture on the electromagnetic shielding property of magnesium alloy, *Mater. Let.* **157**, 73-76 (2015).
- [20] H. Paul, M.M. Miszczyk, A. Gałka, R. Chulist, Z. Szulc, Microstructural and Chemical Composition Changes in the Bonding Zone of Explosively Welded Sheets, *Arch. of Met. and Mat.* **64** (2), 683-694 (2019).
- [21] F. Findik, Recent developments in explosive welding, *Mater. Des.* **32**, 1081-1093 (2011).
- [22] D.M. Fronczek, J. Wojewoda-Budka, R. Chulist, A. Sypien, A. Korneva, Z. Szulc, N. Schell, P. Zieba, Structural properties of Ti/Al clads manufactured by explosive welding and annealing, *Mater. Des.* **91**, 80-89 (2016).
- [23] T. Fras, I. Szachogluchowicz, L. Śnieżek, Ti6Al4V-AA1050-AA2519 explosively-cladded plates under impact loading, *Europ. Phys. J. Spec. Top.* **227**, 17-27 (2018).
- [24] D. Boroński, M. Kotyk, P. Maćkowiak, L. Śnieżek, Mechanical properties of explosively welded AA2519-AA1050-Ti6Al4V layered material at ambient and cryogenic conditions, *Mater. Des.* **133**, 390-403 (2017).
- [25] R. Mola, S. Mróz, P. Szota, S. Sawicki, The analysis of the plastic deformation of two-layered magnesium – aluminium alloys (AZ31 – Al), *Metallurg.* **55** (4), 625-627 (2016).
- [26] S. Mróz, P. Szota, A. Stefanik, FE and physical modelling of plastic flow the two-layer Mg/Al materials, *Comp. Meth. in Mater. Sc.* **17** (3), 148-155 (2017).
- [27] F.H. Norton, *Creep of steel at high temperature*, McGraw Hill, New York, 1929.
- [28] N.J. Hoff, Approximate analysis of structures in the presence of moderately large steps deformation, *Quart. Appl. Mech.* **2**, 49 (1954).
- [29] S. Mróz, *Teoretyczno-technologiczne podstawy walcowania prętów bimetalowych w wykrojach*, Seria Monografie nr 45, Częstochowa, 2015.
- [30] A. Gontarz, A. Dziubińska, Ł. Okoń, Determination of Friction Coefficients at Elevated Temperatures for some Al, Mg and Ti Alloys, *Arch. Metall. Mater.* **56** (2), 379-384 (2011).
- [31] R. Mola, S. Mroz, P. Szota, Effects of the process parameters on the formability of the intermetallic zone in two-layer Mg/Al materials, *Arch. of Civ. and Mech. Eng.* **18** (4), 1401-1409 (2018).